Activation of AKT1 enhances the capacity of senescent BMSCs to regulate osteoclast activation

CHUAN LU[1], XINGGUO PENG[1], BINBIN ZHANG[1], QI YAN[1], BIN DOU[1], GABRIELE KARANIS[2,3], WENZHUO GU[1], PANAGIOTIS KARANIS[3,4] and KEWEN LI[1]

[1]Department of Orthopedics and Joint Surgery, Qinghai University Affiliated Hospital, Qinghai University, Xining, Qinghai 810000, P.R. China; [2]Praxis Pekar, D-59939 Olsberg, Germany; [3]Department of Basic and Clinical Sciences, University of Nicosia Medical School, 2414 Nicosia, Cyprus; [4]Faculty of Medicine, University of Cologne, D-50923 Cologne, Germany

Received February 3, 2025; Accepted July 11, 2025

DOI: 10.3892/mmr.2025.13642

Abstract. Senescent bone mesenchymal stromal cells (BMSCs) play an essential role in bone homeostasis imbalance in osteoporosis; however, the mechanisms through which they regulate osteoclast activation remain unclear. In the present study, highly expressed genes in BMSCs from patients with osteoporosis group were screened using transcriptomic data from the GSE35959 dataset. Subsequently, the *AKT1, MAPK3, RELA* and colony stimulating factor 1 genes were found to be linked to the PI3K/AKT and MAPK signaling pathways and osteoclast differentiation following Gene Ontology and Kyoto Encyclopedia of Genes and Genomes analyses. Principal component analysis revealed a distinct clustering of samples by age and disease status. Gene Set Enrichment Analysis further identified significant enrichment of the PI3K/AKT signaling pathway in osteoporosis progression. Considering the notable involvement of the PI3K/AKT signaling pathway in various cellular ageing processes, *AKT1* was prioritized for further investigation. Analysis of a replicative ageing model of mouse BMSCs showed that AKT1 protein expression was increased in senescent BMSCs and that overexpression of *AKT1* accelerated the initiation of replicative senescence in this model. Finally, the expression levels of osteoclast differentiation markers (receptor activator of nuclear factor κB, nuclear factor of activated T cells, cytoplasmic 1 and tumor necrosis factor receptor-associated factor 6) were assessed using tartrate-resistant acid phosphatase staining. The results from the present study suggested that *AKT1* plays a role in fostering the replicative senescence of BMSCs and that *AKT1* activation in senescent BMSCs contributes to osteoclast differentiation. To the best of the authors' knowledge, the present study is the first to demonstrate that AKT1 upregulation in BMSCs with replicative ageing exacerbates senescence and enhances osteoclast differentiation, offering a novel mechanistic insight into senile osteoporosis.

Correspondence to: Professor Kewen Li, Department of Orthopedics and Joint Surgery, Qinghai University Affiliated Hospital, Qinghai University, 29 Tongren Road, Xining, Qinghai 810000, P.R. China
E-mail: lkwtx68@126.com

Abbreviations: BMSCs, bone mesenchymal stromal cells; TRAP, tartrate-resistant acid phosphatase; SASP, senescence-associated secretory phenotype; MSCs, mouse BMSCs; SA-β-gal, senescence-associated β-galactosidase; RANK, receptor activator of nuclear factor κ B; NFATc1, nuclear factor of activated T cells, cytoplasmic 1; CSE, cystathionine γ-lyase; TRAF6, tumor necrosis factor receptor-associated factor 6; SHIP1, src homology 2 domain-containing inositol 5-phosphatase 1

Key words: osteoporosis, *AKT1*, bone mesenchymal stromal cells, senescence, osteoclast

Introduction

Osteoporosis is a systemic skeletal disorder closely related to ageing, which is characterized by changes in bone structure and the loss of bone density (1). According to the International Osteoporosis Foundation 2024 report (2), ~500 million individuals aged 50 years and older worldwide are affected by osteoporosis, with 37 million fragility fractures occurring annually (equivalent to 70 fractures per minute). This includes over 10 million hip fractures, a subset of fragility fractures that account for significant morbidity and mortality (3). Hence, investigating the pathogenesis of osteoporosis in older individuals is important in the search for novel intervention strategies and treatment modalities.

Cellular ageing is a complex biological process. As the normal cell passage time increases, the mitotic activity decreases and genomic instability increases, leading to cell degradation, fragment accumulation and gradual ageing (4). A study has shown that, as primary cells continue to divide, telomeres shorten. When telomere DNA shortens to a certain extent, cells reach the limit of normal cell division and then automatically initiate an ageing process termed cellular replicative ageing (5). A number of classical signaling pathways regulate the ageing process of bone mesenchymal stromal cells (BMSCs). For instance, research findings have shown that micro RNA (miR)-34a can activate the sirtuin 1/FOXO3a pathway and induce the ageing of BMSCs under hypoxia and serum deficiency (6). Xiang *et al* (7) found that the AKT/FOXO3a/PTEN-induced kinase 1/Parkin axis

suppresses the mitosis-induced senescence of BMSCs. In addition, signaling pathways such as p53/p21$^{WAF1/CIP1}$ (8), p16/retinoblastoma (9), AKT/mTOR (10) and MAPK (11) are associated with cellular senescence. These signaling pathways universally participate in the cellular senescence process of BMSCs. Senescence-related signaling pathways in BMSCs may be a potential target for small molecule inhibitors, thereby preventing and treating age-related degenerative diseases.

BMSCs have the potential to self-replicate and differentiate into multiple cell types, including osteoblasts and adipocytes (12). Age-related functional changes in BMSCs play an essential role in the onset and progression of osteoporosis (13). It has been shown that the senescence-associated secretory phenotype (SASP) secreted by BMSCs increases with age. This secretion includes various biologically active substances that modify the functionality of stem and progenitor cells (14). Tian *et al* (15) found that a reduction in crystallin αB expression can facilitate the degradation of ferritin heavy chain 1, leading to elevated iron-induced cell death in BMSCs and a decline in osteogenic differentiation. Multinucleated osteoclasts are formed by the fusion of monocyte and macrophage progenitor cells and play a critical role in osteoporosis initiation. The functional imbalance between osteoblasts and osteoclasts is a significant contributing factor to osteoporosis (16). A notable study by Ma *et al* (17) found that BMSCs can affect the differentiation of osteoclasts, a process important in maintaining bone metabolism equilibrium. Recent research indicates that the high-fat diet-induced senescence of BMSCs impacts their proliferation and osteogenic capacity, thereby contributing to the development of osteoporosis (18). A prior study on ageing BMSCs have mainly focused on their impact on osteoblast and adipocyte differentiation (19). However, the precise mechanisms through which ageing BMSCs influence osteoclast differentiation in age-related osteoporosis remains ambiguous and necessitates additional investigation.

The primary objective of the present study was to identify genes with high expression levels in bone marrow mesenchymal stem cells (BMSCs) of osteoporosis patients. Initially, the GSE35959 transcriptome sequencing dataset was analyzed. Subsequently, Gene Ontology (GO) and Kyoto Encyclopedia of Genes and Genomes (KEGG) functional enrichment analyses were performed to annotate gene functions and signaling pathways. Principal component analysis (PCA) was then conducted to visualize sample variations and groupings, providing insights into inter-sample differences. Gene set enrichment analysis (GSEA) was employed to determine the enrichment of predefined gene sets associated with cellular processes, exploring potential biological implications at the gene set level. Furthermore, a replicative senescence model of mouse BMSCs was established. Reverse transcription-quantitative (RT-q) PCR and western blotting were utilized to detect the expression of AKT1 at both mRNA and protein levels in senescent BMSCs. Gain-of-function experiments were carried out by overexpressing AKT1 in young BMSCs. To investigate the effects of AKT1 on BMSC senescence and osteoclast activation, activated senescent BMSCs were co-cultured with osteoclast precursors and osteoclast formation was quantified. Through these comprehensive approaches, the present study aimed to identify novel targets for the prevention and treatment of age-related osteoporosis.

Materials and methods

Differential gene screening in BMSCs from elderly individuals diagnosed with osteoporosis. The transcriptome sequencing data from the GSE35959 dataset were downloaded from the Gene Expression Omnibus database (https://www.ncbi.nlm.nih.gov/geo/) (20). In this analysis, the population was divided into three groups, G1 (42-67 year healthy control group, mean age 57.6±9.56 years), G2 (79-89 year non-osteoporotic control group, mean age 81.75±4.86 years) and G3 (79-94 year osteoporosis patient group, mean age 86.2±5.89 years), as shown in Table I. Subsequently, the differential gene expression in the BMSCs from G2 and G3 in the dataset was analyzed. Differential analysis was conducted using the 'limma' package (v3.40.2; https://bioconductor.org/packages/3.10/bioc/html/limma.html) in R software (v4.0.3) (21), selecting results with |log2fold-change (FC)|≥1 and Padj<0.05 as differential genes. Volcano plots were drawn using the 'ggplot2' package (v3.3.5; https://cran.r-project.org/package=ggplot2) in R. Additionally, the expression of differentially expressed genes was visualized through the 'pheatmap' package (v1.0.12; https://cran.r-project.org/package=pheatmap) in R.

GO and KEGG enrichment analyses. The R software package, 'clusterProfiler' (v3.18.0; https://bioconductor.org/packages/3.12/bioc/html/clusterProfiler.html) was used to perform GO and KEGG enrichment analyses on the downregulated genes in the BMSCs from G2 and to visualize the results in a bubble chart form.

PCA and GSEA. The R software package 'ggplot2' (v3.3.5) was used to perform PCA visualization on the gene expression data from three groups (G1, G2 and G3) and to present the results in both two-dimensional (PC1 vs. PC2) and three-dimensional (PC1 vs. PC2 vs. PC3) scatter plot formats. The R software packages 'clusterProfiler' (v3.18.0) and 'fgsea' (v1.16.0; https://bioconductor.org/packages/3.12/bioc/html/fgsea.html) were used to perform GSEA on the differentially expressed genes between G2 and G3, calculate enrichment scores (ES), conduct pathway-related analyses using signaling pathways in the KEGG pathway database and visualize the results via enrichment plots and running enrichment score plots.

Cell lines. Mouse BMSCs were acquired through primary isolation from mouse bone marrow tissue by a subsidiary of the Eli Lilly and Company (Sichuan Lilaisinuo Biotechnology Co., Ltd.) (cat. no. LL-A1-80093). Cell lines were obtained as commercially prepared primary cells or cell lines, without additional animal procurement or primary isolation by the research team. RAW 264.7 cells (cat. no. CL-0190) were procured from Procell Life Science & Technology Co., Ltd.

Establishment of a replicative ageing BMSCs model. Primary BMSCs were cultured in DMEM/F12 medium (Gibco; Thermo Fisher Scientific, Inc.) supplemented with 10% fetal bovine serum (FBS; Gibco; Thermo Fisher Scientific, Inc.; cat. no. 16000-044) and 1% penicillin-streptomycin (Gibco; Thermo Fisher Scientific, Inc.). All cells were maintained at 37˚C with 95% humidity and 5% CO_2 and regularly tested for mycoplasma by PCR (Genlantis Diagnostics Inc.). Based on

Table I. Population grouping in the present study.

Group	Average age (years)	Osteoporosis status	Dataset number	Age, years
G1	57.6±9.56	None	GSM878095	42
			GSM878096	67
			GSM878097	61
			GSM878098	62
			GSM878099	56
G2	81.75±4.86	None	GSM878100	79
			GSM878101	79
			GSM878102	80
			GSM878103	89
G3	86.2±5.89	Present	GSM878104	79
			GSM878105	94
			GSM878106	87
			GSM878107	82
			GSM878108	89

established replicative ageing models, the P3 (early passage) and P10 (late passage) timepoints were selected for analysis, as P10 BMSCs are known to exhibit elevated senescence markers (22,23). The cells were continuously passaged for 10 generations to generate the replicative ageing cell model (P10-BMSCs).

Western blotting (WB). The mouse BMSC samples were collected and then lysed using RIPA buffer supplemented with protease inhibitor and phosphatase inhibitor (all Biosharp Life Sciences). The protein concentration was detected using a BCA protein detection kit (Shanghai Biyuntian Biotechnology Co., Ltd.). Next, ~30 μg of protein sample was separated on a Bis-Tris 10% high-resolution precast gel (Shanghai Yeasen Biotechnology Co., Ltd.) and then transferred onto an Immobilon PSQ PVDF membrane (MilliporeSigma). The membrane was subsequently incubated with 5% skimmed milk (Wuhan Servicebio Technology, Co., Ltd.) for 1 h at room temperature. The membrane was then incubated with primary antibodies against AKT1 (ABclonal Biotech Co., Ltd.; cat. no. A17909; 1:1,000), p16 (ABclonal Biotech Co., Ltd.; cat. no. A23882; 1:1,000), p21 (Proteintech Group, Inc.; cat. no. 28248-1-AP, 1:2,000) and β-actin (ABclonal Biotech Co., Ltd.; cat. no. AC026; 1:50,000) overnight at 4˚C. After washing, the membrane was incubated with a Goat Anti Rabbit IgG (H+L) HRP-conjugated secondary antibody (Affinity Biosciences; cat. no. S0001; 1:5,000) at room temperature for 1 h. Finally, protein bands were visualized using the 'Torchlight' Hypersensitive ECL Western HRP Substrate (Chengdu Zen-Bioscience Co., Ltd.; cat. no. 17046) and imaged using a 5200 Multi chemiluminescence image analysis system (Tanon Science and Technology Co., Ltd.). Densitometric analysis of the bands was performed using Gel-Pro Analyzer software (version 4.0; Media Cybernetics, Inc.).

RNA isolation and RT-qPCR. Total RNA was extracted from mouse sample cells using the Molpure® Cell/Tissue Total RNA Kit (Shanghai Yeasen Biotechnology Co., Ltd.). For RNA extraction, cells were lysed with 350 μl lysis buffer LB (supplied in the kit) at a density of 1-5x10^6 cells per sample (the lysate was repeatedly pipetted until no cell clumps were visible). After quantification, 1 μg RNA was reverse transcribed using the PrimeScript RT kit (Baoriyi Biotechnology Co., Ltd.) with a protocol of 37˚C for 15 min followed by 85˚C for 5 sec; this step was performed according to the manufacturer's protocol. qPCR was performed using TB Green® Premix Ex Taq II (Tli RNaseH Plus; Bao Ri Yi Biotechnology Co., Ltd.), with thermocycling conditions as follows: 95˚C for 30 sec (pre-denaturation), followed by 45 cycles of 95˚C for 5 sec (denaturation), 55˚C for 30 sec (annealing) and 72˚C for 30 sec (extension with fluorescence acquisition); qPCR was also performed according to the manufacturer's protocol. The Cq (quantification cycle) values of the samples were detected using QuantStudio Design & Analysis SE Software (Thermo Fisher Scientific, Inc.). GAPDH was used as the reference gene and quantification was performed using the $2^{-\Delta\Delta Cq}$ method (24). All experiments (RNA extraction, cDNA synthesis, and qPCR) were independently replicated three times. The primer sequences used in this experiment are shown in Table II.

Plasmid transfection. Logarithmically growing bone marrow mesenchymal stem cells (BMSCs) were washed with PBS, trypsinized, centrifuged at 250 x g for 5 min at room temperature, resuspended in culture medium, counted, adjusted to 1x10^5 cells/ml and seeded at 2 ml/well in 6-well plates. After adhesion, transfection complexes were prepared by adding 15 μg AKT1 cDNA recombinant plasmid [pcDNA3.1(+); plasmid (Invitrogen; Thermo Fisher Scientific, Inc.) containing mouse AKT1 ORF sequence (cat. no. MG50254-M; Sino Biological Inc.)] to 300 μl Opti-MEM I in one tube and 30 μl Lipofectamine® 2000 (Invitrogen; Thermo Fisher Scientific, Inc.) to 300 μl Opti-MEM I in another, incubating both for 5 min, combining them, incubating for 10 min and adjusting the volume to 6 ml with Opti-MEM I. Control cells (NC group) were transfected with 15 μg empty cloning vector (Sino Biological Inc.). After 6 h at 37˚C, the medium was replaced

Table II. Primer sequences used in the present study.

Primer	Forward primer, 5'-3'	Reverse primer, 5'-3'
β-actin	CTACCTCATGAAGATCCTGACC	CACAGCTTCTCTTTGATGTCAC
AKT1	TGCACAAACGAGGGGAATATAT	CGTTCCTTGTAGCCAATAAAGG
NFATc1	GAGAATCGAGATCACCTCCTAC	TTGCAGCTAGGAAGTACGTCTT
RANK	CTGAAAAGCACCTGACAAAAGA	CTGTGTAGCCATCTGTTGAGTT
TRAF6	GAAAATCAACTGTTTCCCGACA	ACTTGATGATCCTCGAGATGTC

with a complete medium (cat. no. CM-M131; Procell Life Science & Technology Co., Ltd.), and the cells underwent further culturing such that the total duration from transfection to subsequent experiments was 48 h. For validation, supernatants were collected, cells were washed with PBS, trypsinized, centrifuged at 250 x g for 5 min at room temperature, washed again with PBS and centrifuged at 250 x g for 5 min at room temperature to obtain cell pellets for qPCR and western blot analysis.

Senescence-associated β-galactosidase (SA-β-gal) staining. Logarithmically growing RAW264.7 cells were dissociated into a single-cell suspension, centrifuged at 250 x g for 5 min at room temperature and resuspended in culture medium. Cells were counted and seeded at $0.5x10^5$ cells/ml (2 ml/well) in 6-well plates, then incubated at 37˚C with 5% CO_2. After adhesion, transfection complexes were prepared by mixing 15 μg of AKT1 cDNA ORF Clone (plasmid backbone: Cloning Vector; cat. no. MG50254-M; Sino Biological Inc.) in 300 μl Opti-MEM I Reduced Serum Medium (Gibco; Thermo Fisher Scientific, Inc.) with 30 μl Lipofectamine® 2000 (Invitrogen; Thermo Fisher Scientific, Inc.) in 300 μl Opti-MEM I, incubating both tubes for 5 min, combining them and further incubating for 10 min. The mixture was adjusted to 6 ml with Opti-MEM I before adding to cells. Control cells (NC group) were transfected with an equal mass of empty cloning vector. After 48 h, cells were washed with PBS, fixed with 1 ml β-galactosidase staining fixative (Beyotime Institute of Biotechnology; C0602) for 15 min at room temperature and washed twice with PBS (3 min each). Staining working solution (1 ml/well) was prepared by mixing 10 μl β-galactosidase staining solution A, 10 μl solution B, 930 μl solution C and 50 μl X-Gal solution (Beyotime Institute of Biotechnology; cat. no. C0602) and applied to cells overnight at 37˚C. Images were captured using an inverted biological microscope (DMI1; Leica Microsystems, Ltd.).

Osteolysis induction and co-culturing of RAW264.7 cells and osteoclasts. Logarithmically growing RAW264.7 cells were dissociated into a single-cell suspension, centrifuged at 250 x g for 5 min at room temperature, resuspended in culture medium, counted, adjusted to $0.5x10^5$ cells/ml and seeded at 2 ml/well ($1x10^5$ cells/well) in 6-well plates. After adhesion, cells were induced to differentiate into osteoclasts with α-MEM medium (cat. no. 41061029; Gibco; Thermo Fisher Scientific, Inc.) supplemented with 50 μg/l RANK ligand (cat. no. C28A; Novoprotein Scientific Inc.), incubated at 37˚C in a 5% CO_2 atmosphere and the medium was replaced every 2 days for 5 days. Transfected BMSCs were then counted, adjusted to $2x10^5$ cells/ml and 2 ml/well ($4x10^5$ cells/well) were seeded into the upper chamber of a Transwell plate, while the induced osteoclasts remained in the lower chamber of the 6-well plate for 48 h of co-culture under the same conditions before subsequent staining.

Tartrate-resistant acid phosphatase (TRAP) staining. After removing the supernatant, co-cultured cells were fixed with 4% paraformaldehyde for 15 min at room temperature and washed three times with distilled water. Cells were permeabilized with 0.2% Triton X-100 at room temperature for 30 min, followed by three light washes with distilled water. The TRAP staining kit (cat. no. G1492; Beijing Solarbio Science & Technology Co., Ltd.) was used according to the manufacturer's instructions. Mature osteoclasts were identified as multinucleated cells (≥3 nuclei) and images were captured using an inverted biological microscope (DMI1; Leica Microsystems, Ltd.) (25).

Statistical analysis. GraphPad Prism 8.0 statistical software (Dotmatics) was used to perform graphical analysis and statistical testing on experimental data, which are expressed as the mean ± standard deviation. For experimental datasets, comparisons between two groups were conducted using an unpaired two-tailed Student's t-test. For comparisons among three or more groups, one-way analysis of variance was used for normally distributed data with homogeneous variances, followed by Tukey's Honestly Significant Difference test for pairwise comparisons when overall differences were significant, and Kruskal-Wallis test was applied to non-normally distributed or heteroscedastic data, with Dunn's multiple comparisons test for post hoc pairwise comparisons upon significant differences. For bioinformatics data analyses (such as high-throughput sequencing or -omics data), R software 4.2.2 was used to handle complex statistical modeling and computational pipelines. $P<0.05$ was considered to indicate a statistically significant difference.

Results

Screening of differentially expressed genes in BMSCs from G3. The GSE35959 dataset was selected to analyze the effects of primary osteoporosis on BMSC gene expression. Initially, no abnormal outliers were observed in the BMSC samples from G2 and G3 (Fig. 1A). Subsequently, the differential gene expression between BMSCs from G2 and G3 was analyzed. According to the results, BMSCs obtained from G2 had 274 upregulated genes and 2,592 downregulated genes (Fig. 1B).

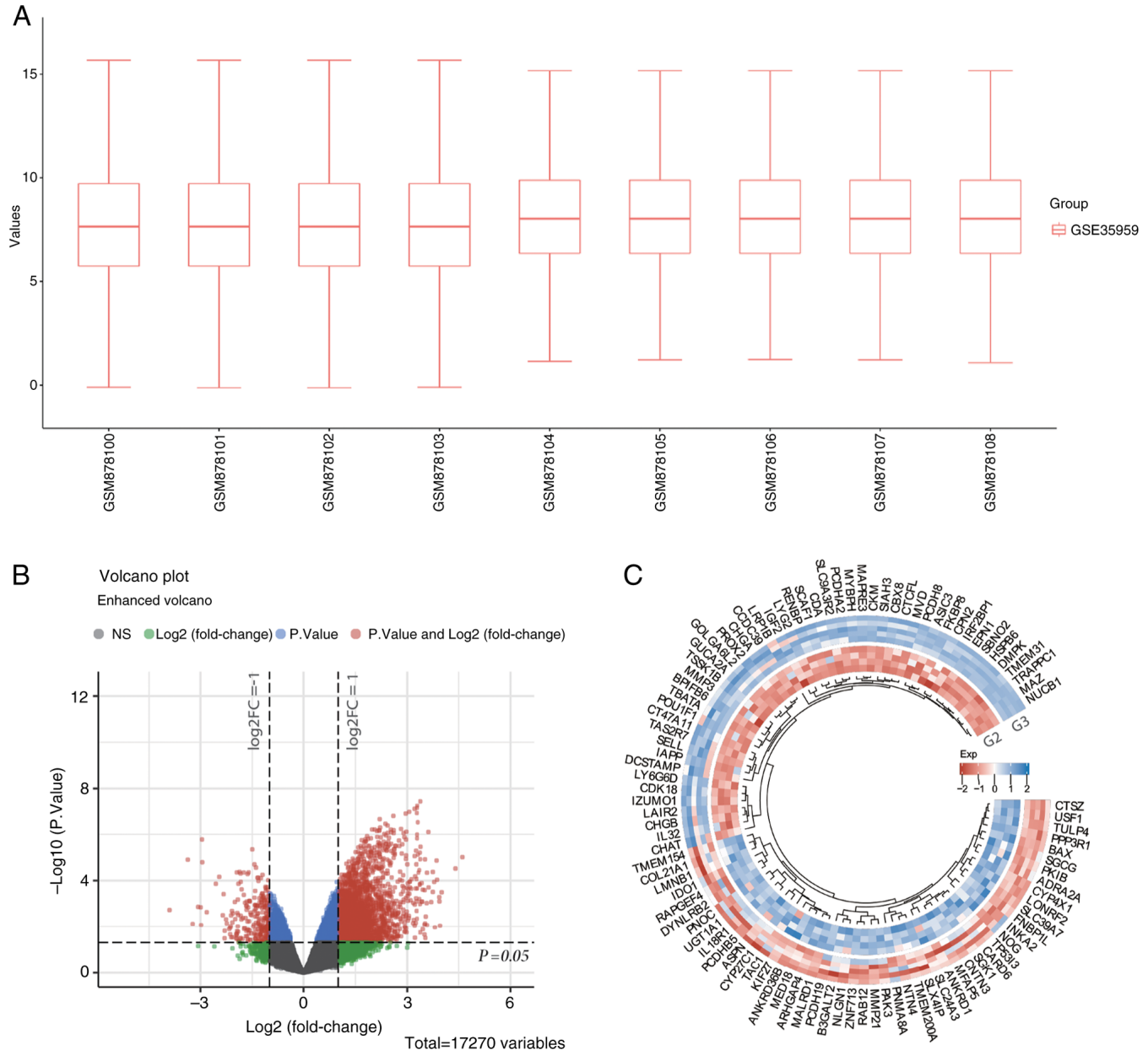

Figure 1. Differential gene screening in BMSCs from G2 (79-89 year non-osteoporotic control group, mean age 81.75±4.86 years) and G3 (79-94 year osteoporosis patient group, mean age 86.2±5.89 years). (A) Normalization of the expression in the GSE35959 samples. (B and C) Volcano and volcano maps of the differential genes. In the schematic, the outermost circle represents the samples selected in G3 and the innermost circle represents the samples selected in G2. The dendrogram represents the clustering visualization results of the differentially expressed genes. BMSCs, bone mesenchymal stromal cells.

The heatmap shown in Fig. 1C depicts the expression of the differentially expressed genes in the two groups. Due to the large number of differentially expressed genes, the top 50 upregulated and the top 50 downregulated genes with the greatest differential changes are displayed separately.

GO and KEGG enrichment analyses. GO and KEGG enrichment analyses were performed on the 2,592 genes that were upregulated in BMSCs from G3. The GO results showed that these genes mainly participate in processes such as 'striated muscle cell differentiation,' 'regulation of trans-synaptic signaling' and 'regulation of neurotransmitter levels' (Fig. 2A). The KEGG enrichment analysis revealed a significant association with the 'PI3K/Akt signaling pathway', 'osteoclast differentiation' and 'MAPK signaling pathway' (Fig. 2B). Several classical signaling pathways, including PI3K/AKT/mTOR, p53/p21 and MAPK, have been demonstrated to influence BMSC ageing (26,27). Subsequent analysis indicated the enrichment of *AKT1*, *MAPK3*, *RELA* and *CSF1* in the MAPK signaling, PI3K/AKT signaling and osteoclast differentiation pathways. Subsequently, using the GSE35959 dataset, the levels of the aforementioned four genes in BMSCs from G1, G2 and G3 were further analyzed (Fig. S1). According to the results, the expression levels of the four genes were markedly lower in BMSCs from G2 than those from G1, while the expression levels of the four genes were markedly higher in BMSCs from G3 than those from G1. Hence, it was hypothesized that the overactivation of *AKT1*, *MAPK3*, *RELA*

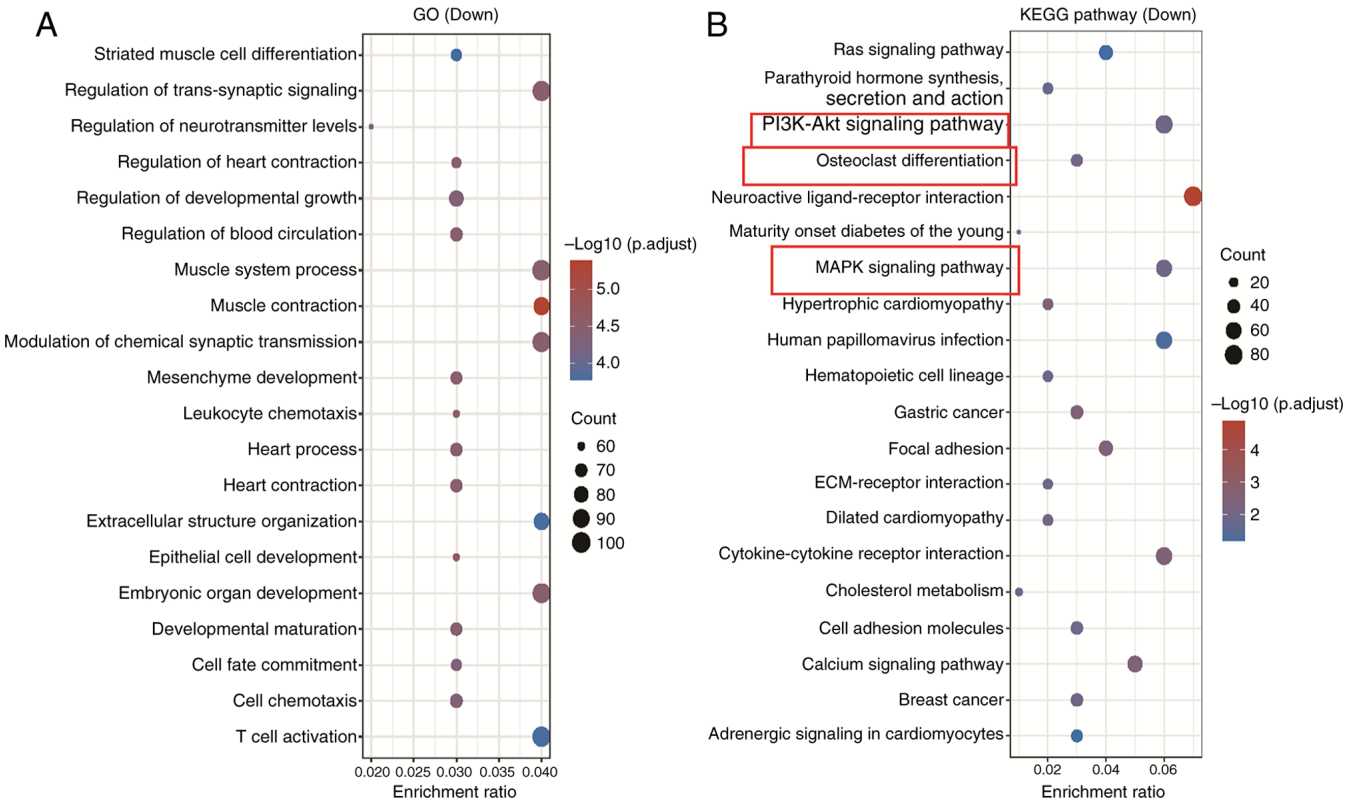

Figure 2. GO and KEGG enrichment analyses. (A) GO and (B) KEGG analyses of the highly expressed genes in BMSCs from G3 (79-94 year osteoporosis patient group, mean age 86.2±5.89 years). GO, Gene Ontology; KEGG, Kyoto Encyclopedia of Genes and Genomes; BMSCs, bone mesenchymal stromal cells.

and *CSF1* in the stem cells of G3 may contribute to the pathogenesis of osteoporosis.

PCA and GSEA. PCA analysis revealed differences in gene expression patterns between the three groups: G1, G2 and G3. Fig. S2A displays a two-dimensional PCA plot, where PC1 explains 22.4% of the variation and PC2 explains 13% of the variation. The three sample groups form distinct clusters, indicating significant differences in gene expression between them. Fig. S2B shows the three-dimensional PCA plot, adding PC3 (explaining 9.2% of the variation), further reinforcing the separation pattern between the sample groups. This clustering pattern suggests that both age (G1 vs. G2) and disease status (G2 vs. G3) have significant effects on gene expression that can be clearly distinguished through PCA. GSEA revealed significant positive enrichment of the 'KEGG_PI3K-Akt_signaling_pathway' in the comparison between the G3 and G2 groups (Fig. S2C). The normalized enrichment score was 1.552 with an adjusted P-value of 0.004, indicating statistically significant activation of this pathway. The running enrichment score (RES) curve displayed a prominent positive peak (maximum RES ~0.3) and genes within the pathway were predominantly clustered on the left side of the ranked list (red area), reflecting their upregulated expression in the G3 group. These results suggested that the PI3K/AKT signaling pathway is markedly activated during the progression from healthy aging (G2) to osteoporosis (G3). This differential regulation highlights the potential role of this pathway in the pathophysiology of osteoporosis, offering critical insights for identifying therapeutic targets.

Changes in AKT1 expression levels in BMSCs with replicative ageing. In the present study, P3 and P10 denoted early (younger) and late (older) passage numbers of BMSCs, respectively, with higher passage numbers reflecting increased replicative cycles. It is well established that SA-β-gal staining, p21 expression and p16 expression serve as significant biomarkers of the ageing process in BMSCs (28,29). The results indicated that the number of SA-β-gal positive cells was markedly higher in the P10-MSCs group than in the P3-MSCs group ($P<0.0001$). Additionally, the relative protein expression levels of the cell ageing markers, p16 ($P<0.001$) and p21 ($P<0.01$), were also markedly increased in the P10-MSCs group compared with the P3-MSCs group. These results suggested the successful establishment of a replicative ageing model of BMSCs in the P10-MSCs group (Fig. 3A and B).

AKT is a serine/threonine kinase that is dependent on PI3K. Research indicates that the PI3K/AKT/mTOR pathway is essential for regulating cell differentiation (30). As a member of the AKT family, AKT1 is integral to the PI3K/AKT signaling pathway. Consequently, a further examination of the AKT1 expression levels in both the P3-MSCs and the P10-MSCs groups was conducted. The results of the PCR and WB analyses indicated that, compared with the P3-MSCs group, P10-MSCs had markedly higher AKT1 protein and mRNA expression levels ($P<0.05$; Fig. 3C). These findings suggest that replicative ageing may enhance the expression of AKT1 protein in BMSCs.

Confirmation of the transfection efficiency of the AKT1 overexpression plasmid. To further investigate the effect of AKT1

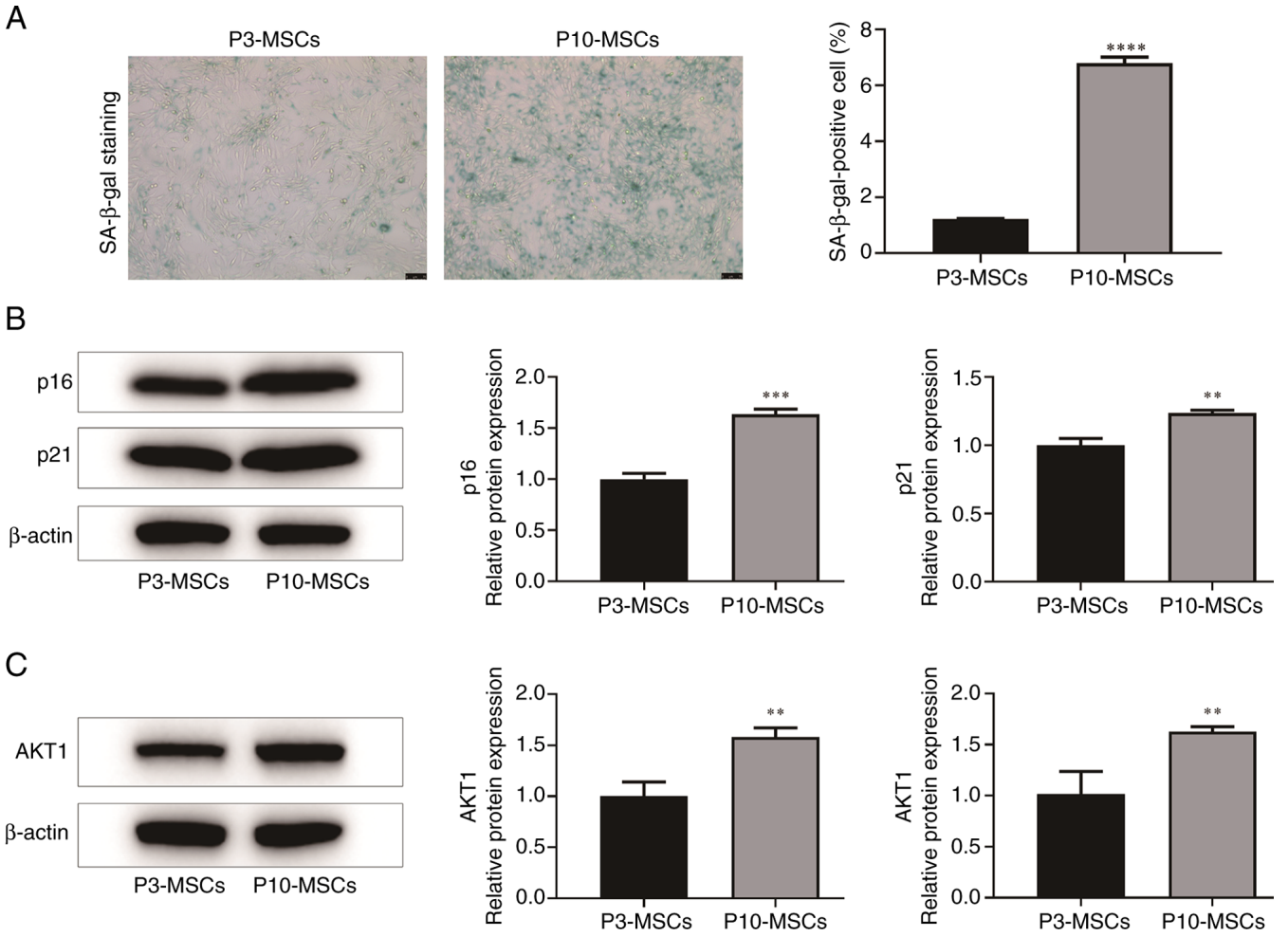

Figure 3. Changes in the AKT1 expression level in replicative-aged BMSCs. (A) SA-β-gal staining to observe cellular senescence. Scale bar, 75 μm. (B) WB detection of the protein expression levels of the cellular senescence markers, p21 and p16, in the P10-MSCs group and P3-MSCs group. (C) WB and PCR were used to detect the relative AKT1 protein and mRNA levels, respectively. **P<0.01, ***P<0.001, ****P<0.0001. BMSCs, bone mesenchymal stromal cells; SA-β-gal, senescence-associated β-galactosidase; WB, western blotting.

on the ageing of BMSCs, the gene encoding the AKT1 protein was cloned into a pcDNA expression vector and subsequently transfected into P10-MSCs. As shown in Fig. 4A, the WB results showed that P10-MSCs transfected with pcDNA AKT1 had higher levels of AKT1 protein. Following statistical analysis of the results, it was found that in transfected P10-MSCs, AKT1 protein levels exhibited a significant increase compared with transfected P3-MSCs (P<0.05). This finding suggests that replicative ageing has a notable effect on elevating AKT1 protein levels in BMSCs. In addition, compared with the P10-MSCs + pcDNA negative control (NC) group, the P10-MSCs + pcDNA AKT1 group exhibited a statistically significant increase in AKT1 protein levels (P<0.0001; Fig. 4B). Finally, qPCR demonstrated that, compared with the P10-MSCs + pcDNA NC group, the relative mRNA expression level of *AKT1* was statistically elevated in the P10-MSCs + pcDNA AKT1 group (P<0.0001; Fig. 4C). In summary, these experimental findings indicated the successful transfection of pcDNA AKT1 into P10-MSCs.

Effect of AKT1 overexpression on the replicative ageing of BMSCs. Subsequently, the effect of *AKT1* overexpression on the replicative ageing of BMSCs was verified. Following SA-β-gal staining, the P10-MSCs + pcDNA AKT1 group had a markedly higher proportion of SA-β-gal positive cells than the P10-MSCs + pcDNA group (Fig. 5A). Subsequently, a comprehensive analysis of the protein levels of the cell ageing markers, p16 and p21, in all four experimental groups was conducted through WB experiments (Fig. 4A). In addition, compared with the P10 MSCs + pcDNA group, the levels of the p16 and p21 proteins were markedly increased in the P10 MSCs + pcDNA AKT1 group (P<0.001; Fig. 5B and C). In conclusion, these findings indicated that the overexpression of *AKT1* promotes the ageing process of BMSCs.

Effect of AKT1 overexpression on regulating osteoclast differentiation in replicative ageing BMSCs. In the aforementioned enrichment analysis, it was indicated that *AKT1* may be markedly associated with the differentiation of osteoclasts in G3. Therefore, experiments using replication-aged BMSCs were performed to further test the regulatory role of *AKT1* in osteoclast differentiation. Initially, the supernatant derived from BMSCs was co-cultured with osteoclasts, as shown in Fig. 6. It was found that the quantity of $TRAP^+$ multinucleated cells in the P10-MSCs group was higher than that in the P3-MSCs

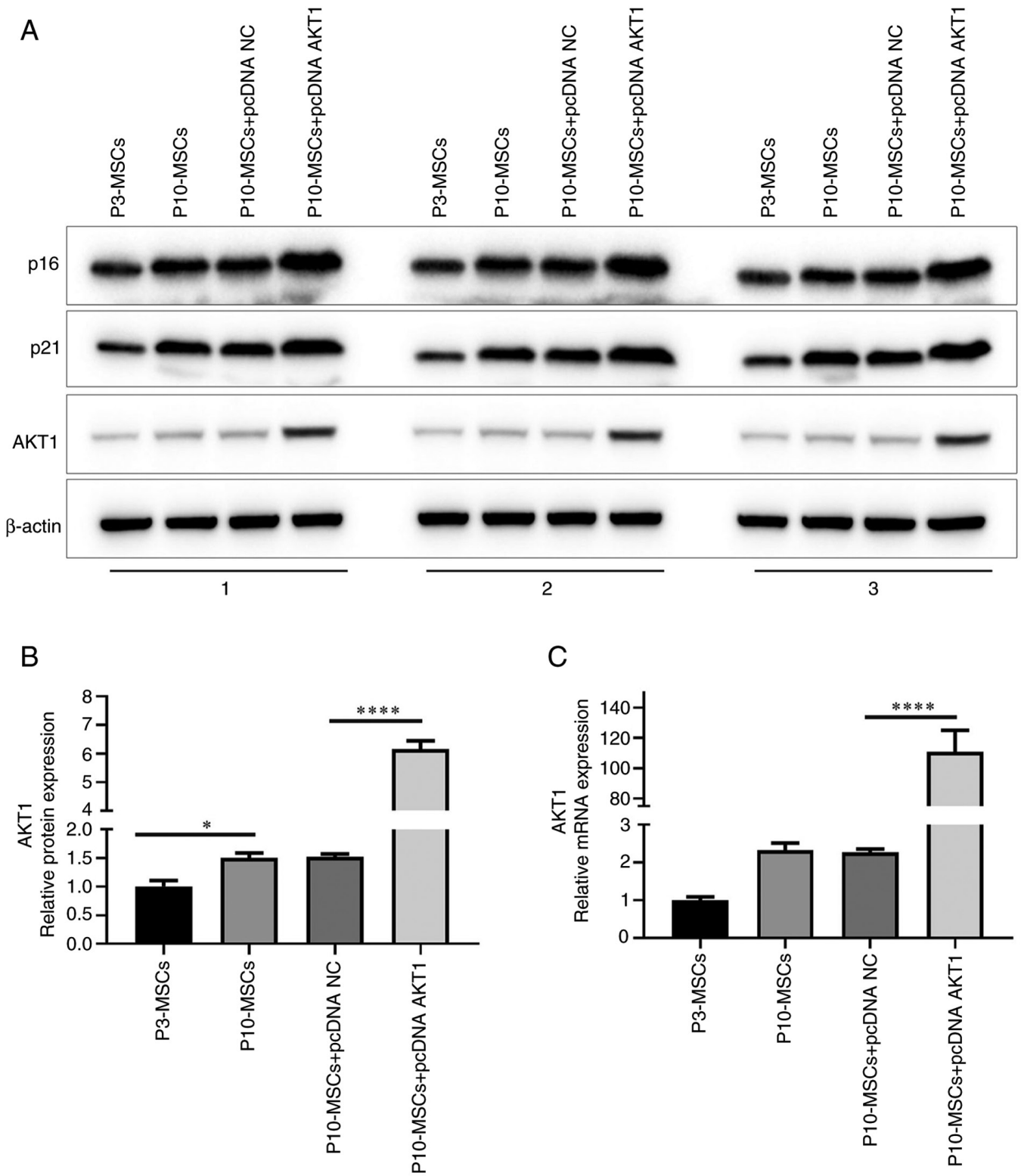

Figure 4. Overexpression efficiency of AKT1 was detected by WB and PCR. (A) Detection of the protein expression levels of AKT1, p16 and p21 through WB. (B) AKT1 protein expression in the four groups (P10-MSCs, P3-MSCs, P10-MSCs + pcDNA NC and P10-MSCs + pcDNA AKT1). (C) *AKT1* mRNA expression in the four groups (P10-MSCs, P3-MSCs, P10-MSCs + pcDNA NC and P10-MSCs + pcDNA AKT1). *P<0.05, ****P<0.0001. WB, western blotting.

group, but this difference was not statistically significant (P>0.05). Additionally, the P10-MSCs showed a tendency to express osteoclast differentiation markers. The nuclear factor of activated T cells, cytoplasmic 1 *(NFATc1)*, tumor necrosis factor receptor-associated factor 6 *(TRAF6)* and *RANK* mRNA levels were higher in P10-MSCs than in the P3-MSCs group, but this difference was not statistically significant (P>0.05). Subsequently, a comparative analysis of the number of TRAP^{+} multinucleated cells and the relative mRNA expression levels of osteoclast differentiation markers, including *NFATc1*, *TRAF6* and *RANK*, between the P10-MSCs group and the P10-MSCs + pcDNA NC

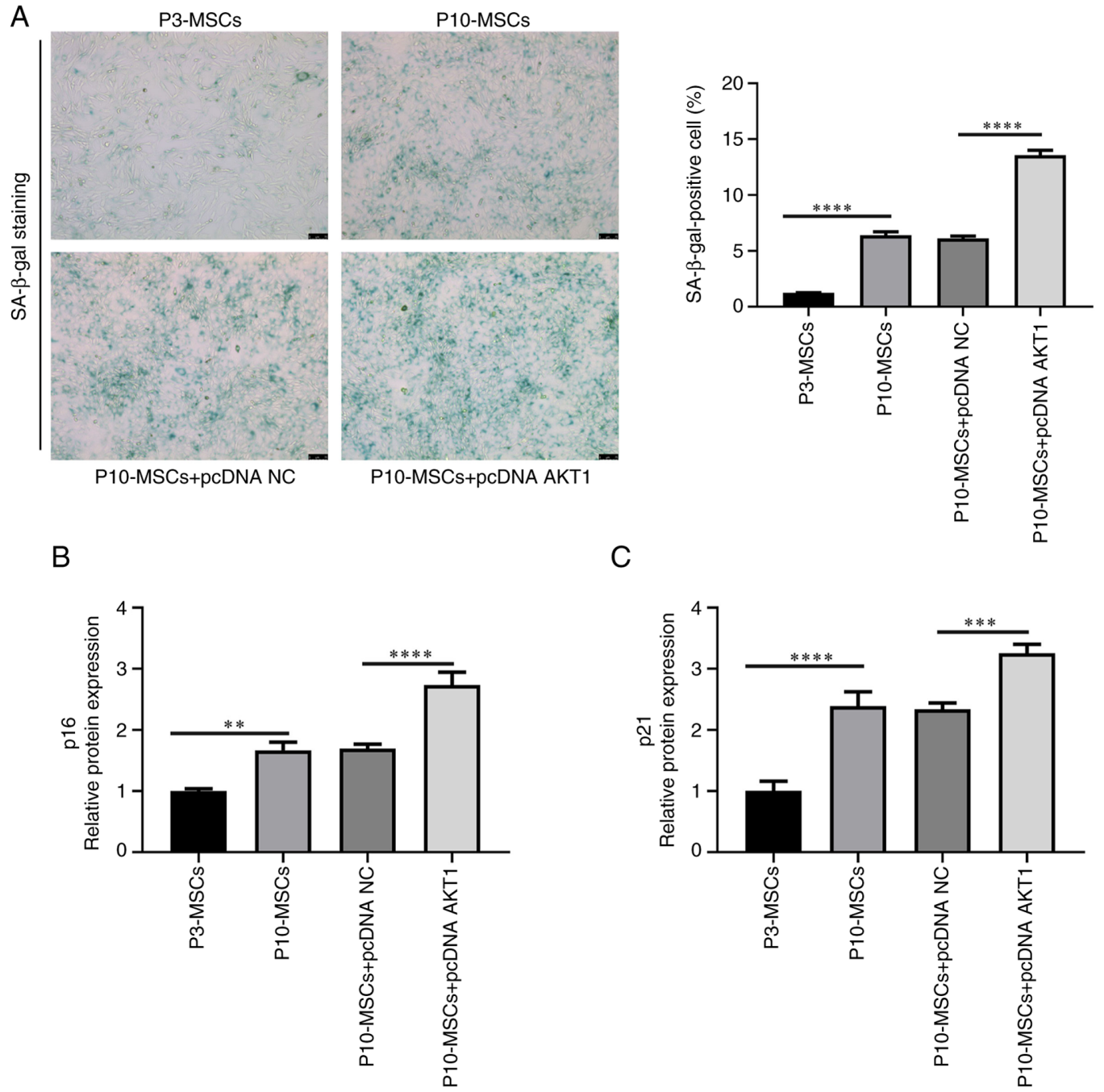

Figure 5. Effect of *AKT1* overexpression on the replicative senescence of BMSCs. (A) SA-β-gal staining to observe cellular senescence. Scale bar, 75 μm. (B and C) Protein expression of the cell ageing markers, p21 and p16, in the four groups (P10-MSCs, P3-MSCs, P10-MSCs + pcDNA NC and P10-MSCs + pcDNA AKT1). **P<0.01, ***P<0.001, ****P<0.0001. BMSCs, bone mesenchymal stromal cells; SA-β-gal, senescence-associated β-galactosidase.

group was conducted. There were no significant differences (P>0.05) in these markers between these groups. However, the results of the PCR experiment indicated that, compared with the P10-MSCs + pcDNA NC group, the relative mRNA expression levels of the osteoclast differentiation markers, *NFATc1* (P<0.01), *TRAF6* (P<0.0001) and *RANK* (P<0.001), were markedly increased in the P10-MSCs + pcDNA AKT1 group. In summary, these findings suggested that BMSCs experiencing replicative ageing may facilitate the differentiation of osteoclasts. Furthermore, an elevated *AKT1* expression level in ageing BMSCs may be associated with the promotion of osteoclast differentiation.

Discussion

Research has demonstrated that the ageing of BMSCs influences the equilibrium between bone formation and resorption, serving as a significant contributor to age-related bone diseases (31). Jin *et al* (32) found that optineurin facilitates the osteogenic differentiation of BMSCs and inhibits adipogenic differentiation by delaying cellular ageing and enhancing autophagy. According to Hu *et al* (22), nucleosome assembly protein 1 like 2 is responsible for driving the ageing of mesenchymal stem cells and preventing their differentiation into osteoblasts. However, current research on the effects of ageing BMSCs in

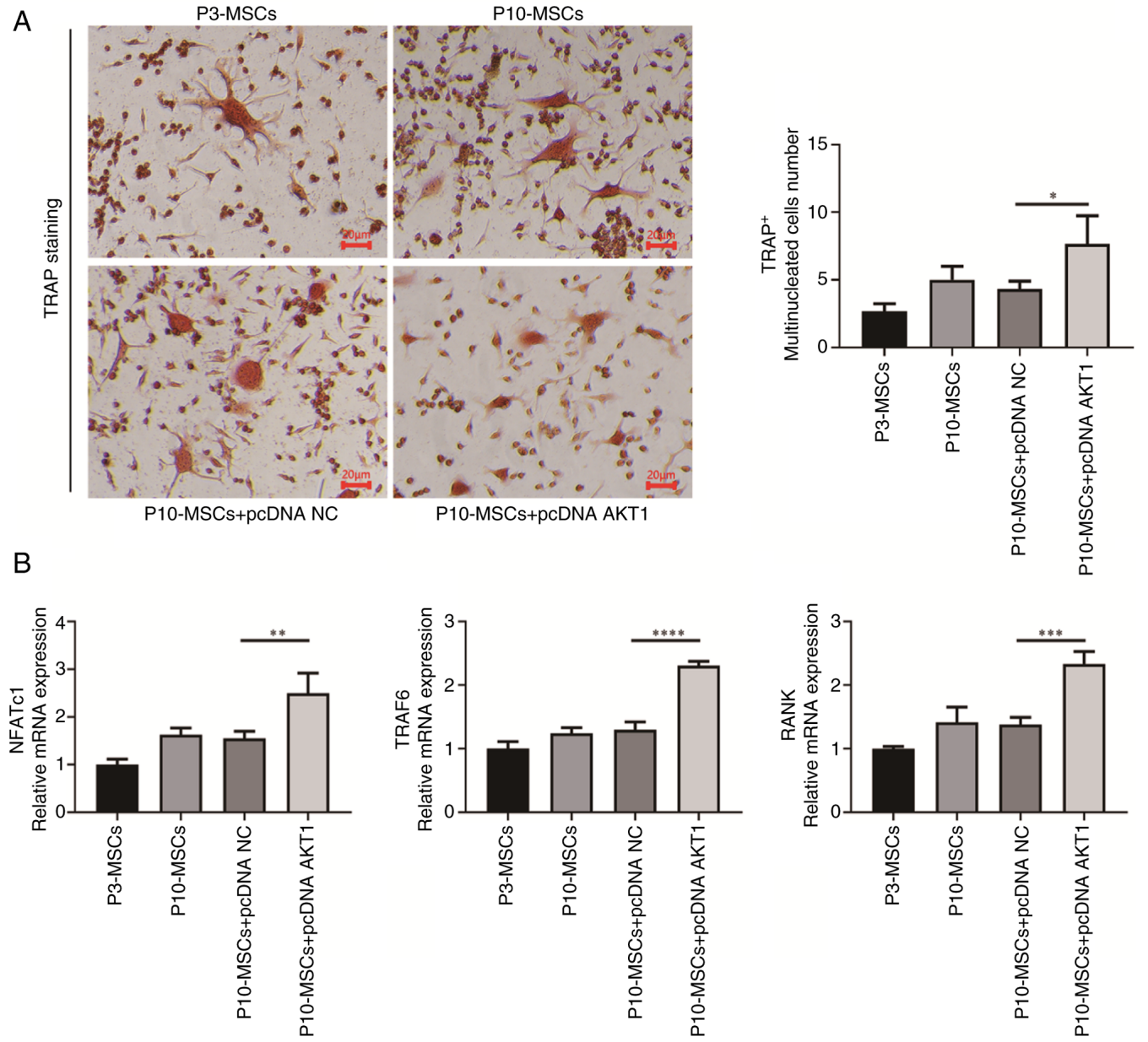

Figure 6. Replicative-aged BMSCs regulate osteoclast differentiation. (A) TRAP staining to detect osteoclast differentiation (x200 magnification). (B) PCR to detect the mRNA expression of the osteoblast markers, *NFATc1*, *TRAF6* and *RANK*, in each group. *P<0.05, **P<0.01, ***P<0.001, ****P<0.0001. BMSCs, bone mesenchymal stromal cells; TRAP, tartrate-resistant acid phosphatase; NFATc1, nuclear factor of activated T cells, cytoplasmic 1; TRAF6, tumor necrosis factor receptor-associated factor 6; RANK, receptor activator of nuclear factor κB.

age-related bone diseases predominantly emphasizes the differentiation processes between osteoblasts and adipocytes. By contrast, there is a paucity of studies investigating the influence of ageing BMSCs on osteoclast differentiation. Ageing BMSCs can promote the differentiation of bone marrow monocytes into osteoclasts, ultimately leading to the occurrence of osteoporosis (33). Research on the novel mechanisms that ageing BMSCs use to influence osteoclast activation is essential for age-related osteoporosis discovery, prevention and treatment. In the present study, it was observed that replicative ageing enhanced the expression of AKT1 protein in BMSCs and this increase in AKT1 expression further exacerbated the ageing process of BMSCs. Furthermore, the overexpression of AKT1 was shown to promote osteoclast activation in ageing BMSCs, which may contribute to the development of osteoporosis.

Previous research has confirmed that cellular ageing is influenced by the regulation of various signaling pathways. For instance, Prince *et al* (34) identified a correlation between the AKT/mTOR pathway and the progression of ageing in ACP epithelial cells. In addition, Li *et al* (35) demonstrated that deoxynivalenol induces cellular senescence in RAW264.7 macrophages through modulation of the hypoxia-inducible factor-1α/p53/p21 signaling pathway. The present study initially conducted a screening of highly expressed genes in BMSCs from G3, using bioinformatics methodologies. Then, an enrichment analysis of the highly expressed genes was conducted. Bubble plots revealed a significant association between these genes and the PI3K/AKT and MAPK signaling pathways, as well as osteoclast differentiation processes. It is noteworthy that the four genes, *AKT1*, *MAPK3*, *RELA* and *CSF1*, exhibited significant

enrichment in the aforementioned three pathways. PCA confirmed transcriptional divergence with aging and disease and GSEA revealed significant enrichment of the PI3K/AKT pathway in G3 vs. G2. Previous research has indicated that AKT is crucial in the ageing process across various cell types (36,37). Nevertheless, there has been a lack of research to ascertain whether the expression of *AKT1* influences the replicative ageing of BMSCs.

Ageing-related biomarkers such as SA-β-gal staining, p21 expression and p16 expression are used to evaluate the process of cellular ageing (38,39). The present study initially observed a significant increase in ageing-related markers, specifically in the p21 and p16 protein levels as well as the number of SA-β-gal positive cells, in the P10-MSCs group (cultured continuously for 10 generations) compared with the P3-MSCs group (cultured for three generations). This indicated that a replicative ageing model was successfully established using P10-MSCs. In addition, it was found that P10-MSCs expressed markedly higher levels of AKT1 mRNA and protein, which indicated that senescent BMSCs have higher AKT1 protein levels. Additionally, the overexpression of *AKT1* in the P10-MSCs group resulted in an increased proportion of SA-β-gal positive cells, as well as higher p21 and p16 levels. This finding suggested that *AKT1* may facilitate the promotion of senescence in BMSCs. Consistent with these findings, the study conducted by Xiang *et al* (7) demonstrated that CSE can induce ageing in BMSCs through the upregulation of phosphorylated AKT. Overall, in the present study, the expression of AKT1 was found to be elevated in senescent BMSCs and the overexpression of AKT1 was shown to promote senescence in these cells. Accordingly, it is hypothesized that *AKT1* represents a novel therapeutic target for treating and preventing replicative senescence in BMSCs. To the best of our knowledge, the present study is the first to indicate that *AKT1* upregulation enhances the regulation of osteoclast differentiation in BMSCs undergoing replicative ageing.

The overactivation of osteoclasts is a significant contributor to the pathogenesis of osteoporosis. A previous study showed that the pro-inflammatory SASP released by senescent cells activates osteoclast precursors to promote osteoclast differentiation, ultimately leading to a decrease in bone density (40). In addition, a study has shown that *CSF1* regulated by nuclear paraspeckle assembly transcript 1 can be delivered extracellularly through paracrine pathways in ageing BMSCs, thereby promoting osteoclast differentiation (41). In the present study, a greater percentage of $TRAP^+$ multinucleated cells was observed in the P10-MSCs group than in the P3-MSCs group, it has been documented that *RANK*, *NFATc1* and *TRAF6* serve as significant biomarkers in the differentiation process of osteoclasts (42,43). The present study found that the *RANK*, *NFATc1* and *TRAF6* mRNA expression levels were increased in P10-MSCs. These findings suggested that ageing BMSCs may facilitate the activation of osteoclasts. Xie *et al* (44) found that the *SHIP1* activator, AQX-1125, modulates the differentiation of osteoblasts and osteoclasts via the PI3K/AKT and NF-κB signaling pathways.

However, there are some shortcomings in the present research. First, further investigation is needed on how the upregulation of *AKT1* promotes the replicative ageing of BMSCs. A previous report has indicated that epigenetics can regulate gene transcription and translation processes by modifying gene expression through various pathways and cellular ageing is regulated by DNA methylation, histone modification, chromatin remodeling and non-coding RNA (45). While the present study links AKT1 upregulation to senescence, the upstream triggers (such as DNA damage and telomere attrition) remain unexplored. Future research should assess AKT1 phosphorylation and its interaction with the PI3K/AKT pathway components to elucidate mechanistic drivers. The present study has certain room for improvement in the construction of the senescence model and mechanistic analysis. The current research only selected two timepoints, passage 3 (early passage) and passage 10 (late passage), to establish the senescence model. While this selection was based on the classical replicative senescence model (where passage 10 BMSCs are known to highly express senescence markers), it indeed failed to fully characterize the continuous trajectory of BMSCs transitioning from a highly proliferative state to degenerative senescence. Such a jump-type analysis between two passages may have obscured key intermediate-stage changes during the senescence process. The present study started from molecular characteristics of clinical senescent samples to validate pathological key pathways, selecting senescent cells as subjects. The role of AKT1 in proliferative cells needs upstream mechanism exploration via independent experiments. AKT1 overexpression may have 'enhancing/inducing senescence' dual effects, with mechanisms needing further study. Expanding this area will aid revealing the role of AKT1 in the senescence continuum and provide early osteoporosis intervention targets. In addition, a recent study found that aldehyde dehydrogenase 2 regulates mesenchymal stem cell ageing by maintaining mitochondrial homeostasis (46), which provides direction for future research. Second, regarding how ageing BMSCs regulate osteoclast differentiation, the study by Yin *et al* (33) demonstrated that the extracellular vesicles containing miR-144-5p secreted by ageing BMSCs play a significant role in osteoclast differentiation but the specific mechanism is unclear. Third, while rigorous thresholds ($|\log2FC|\geq1$, $Padj<0.05$) support the findings of the present study, the limited sample size of the GSE35959 dataset may affect generalizability. Larger-scale studies incorporating broader age ranges are warranted to validate the current observations. Future studies should incorporate functional assays (such as bone resorption pits) to validate the osteoclast-promoting effects of AKT1-overexpressing BMSCs.

In conclusion, the findings of the present study indicated that ageing increased the expression of *AKT1* in BMSCs and this elevated expression of *AKT1* further exacerbates the ageing process. In addition, ageing BMSCs that upregulate *AKT1* can promote osteoclast differentiation. The present study provided new insights into the mechanisms of age-related osteoporosis, as well as potential prevention and treatment targets.

Acknowledgements

Not applicable.

Funding

The present study was supported by the funding of the 'Kunlun Talent Plateau Famous Doctor' Talent Project of Qinghai Province in 2022.

Availability of data and materials

The data generated in the present study are included in the figures and/or tables of this article.

Authors' contributions

CL was responsible for writing the original draft, reviewing and editing, methodology (including design of experimental protocols and analytical approaches) and investigation (acquisition of data). XP contributed to core study conception and design, managed data acquisition, organization, and statistical analysis/interpretation of key results, revised core content (conclusion rigor, discussion depth), reviewed and approved the final publication version, and took responsibility for the work's accuracy and integrity. BZ performed experimental data validation for reliability in addition to data archiving and structured storage. QY focused on experimental quality control (instrument calibration and reagent validation). BD was responsible for validation of the data analysis methods and results, as well as analysis and interpretation of key data. GK was responsible for validation, reviewing, writing and conception of the study design. WG was responsible for validation of the data analysis methods and results, as well as analysis and interpretation of key data. PK was responsible for validation, reviewing, writing and interpretation of experimental data. KL was responsible for resources, supervision, project administration, funding acquisition, and conception and design of the overall study. BD and WG confirm the authenticity of all the raw data. All authors read and approved the final manuscript.

Ethics approval and consent to participate

All procedures, including the use of primary BMSCs, were approved by the Research Ethics Committee of Qinghai University Affiliated Hospital (approval no. P-SL-202481). The extraction of primary BMSCs from mice used in the experiment was approved by the Experimental Animal Ethics Committee of Sichuan Lilaisinuo Biotechnology Co., Ltd. (approval no. LLSN-2023170).

Patient consent for publication

Not applicable.

Competing interests

The authors declare that they have no competing interests.

References

1. Roux C and Briot K: The crisis of inadequate treatment in osteoporosis. Lancet Rheumatol 2: e110-e119, 2020.
2. International Osteoporosis Foundation (IOF): Epidemiology of osteoporosis and fragility fractures. IOF Official Report, 2024. https://www.osteoporosis.foundation/facts-statistics/epidemiology-of-osteoporosis-and-fragility-fractures. Accessed May 21, 2025.
3. Salari N, Darvishi N, Bartina Y, Larti M, Kiaei A, Hemmati M, Shohaimi S and Mohammadi M: Global prevalence of osteoporosis among the world older adults: A comprehensive systematic review and meta-analysis. J Orthop Surg Res 16: 669, 2021.
4. Ogrodnik M: Cellular aging beyond cellular senescence: Markers of senescence prior to cell cycle arrest in vitro and in vivo. Aging Cell 20: e13338, 2021.
5. Zhu Y, Liu X, Ding X, Wang F and Geng X: Telomere and its role in the aging pathways: Telomere shortening, cell senescence and mitochondria dysfunction. Biogerontology 20: 1-16, 2019.
6. Zhang F, Cui J, Liu X, Lv B, Liu X, Xie Z and Yu B: Roles of microRNA-34a targeting SIRT1 in mesenchymal stem cells. Stem Cell Res Ther 6: 195, 2015.
7. Xiang K, Ren M, Liu F, Li Y, He P, Gong X, Chen T, Wu T, Huang Z, She H, *et al*: Tobacco toxins trigger bone marrow mesenchymal stem cells aging by inhibiting mitophagy. Ecotoxicol Environ Saf 277: 116392, 2024.
8. Cheng Y, Wang S, Zhang H, Lee JS, Ni C, Guo J, Chen E, Wang S, Acharya A, Chang TC, *et al*: A non-canonical role for a small nucleolar RNA in ribosome biogenesis and senescence. Cell 187: 4770-4789.e23, 2024.
9. Chicas A, Wang X, Zhang C, McCurrach M, Zhao Z, Mert O, Dickins RA, Narita M, Zhang M and Lowe SW: Dissecting the unique role of the retinoblastoma tumor suppressor during cellular senescence. Cancer Cell 17: 376-387, 2010.
10. Liu G, Li X, Yang F, Qi J, Shang L, Zhang H, Li S, Xu F, Li L, Yu H, *et al*: C-phycocyanin ameliorates the senescence of mesenchymal stem cells through ZDHHC5-mediated autophagy via PI3K/AKT/mTOR pathway. Aging Dis 14: 1425-1440, 2023.
11. Wan D, Ai S, Ouyang H and Cheng L: Activation of 4-1BB signaling in bone marrow stromal cells triggers bone loss via the p-38 MAPK-DKK1 axis in aged mice. Exp Mol Med 53: 654-666, 2021.
12. Gao Q, Wang L, Wang S, Huang B, Jing Y and Su J: Bone marrow mesenchymal stromal cells: Identification, classification and differentiation. Front Cell Dev Biol 9: 787118, 2022.
13. Infante A and Rodríguez CI: Osteogenesis and aging: Lessons from mesenchymal stem cells. Stem Cell Res Ther 9: 244, 2018.
14. Yin Y, Chen H, Wang Y, Zhang L and Wang X: Roles of extracellular vesicles in the aging microenvironment and age-related diseases. J Extracell Vesicles 10: e12154, 2021.
15. Tian B, Li X, Li W, Shi Z, He X, Wang S, Zhu X, Shi N, Li Y, Wan P and Zhu C: CRYAB suppresses ferroptosis and promotes osteogenic differentiation of human bone marrow stem cells via binding and stabilizing FTH1. Aging (Albany NY) 16: 8965-8979, 2024.
16. Gambari L, Grassi F, Roseti L, Grigolo B and Desando G: Learning from monocyte-macrophage fusion and multinucleation: Potential therapeutic targets for osteoporosis and rheumatoid arthritis. Int J Mol Sci 21: 6001, 2020.
17. Ma QL, Fang L, Jiang N, Zhang L, Wang Y, Zhang YM and Chen LH: Bone mesenchymal stem cell secretion of sRANKL/OPG/M-CSF in response to macrophage-mediated inflammatory response influences osteogenesis on nanostructured Ti surfaces. Biomaterials 154: 234-247, 2018.
18. Chen J, Kuang S, Cen J, Zhang Y, Shen Z, Qin W, Huang Q, Wang Z, Gao X, Huang F and Lin Z: Multiomics profiling reveals VDR as a central regulator of mesenchymal stem cell senescence with a known association with osteoporosis after high-fat diet exposure. Int J Oral Sci 16: 41, 2024.
19. Li H, Qu J, Zhu H, Wang J, He H, Xie X, Wu R and Lu Q: CGRP regulates the age-related switch between osteoblast and adipocyte differentiation. Front Cell Dev Biol 9: 675503, 2021.
20. Benisch P, Jakob F and Ebert R: Effects of aging, primary osteoporosis and cellular senescence on human mesenchymal stem cells. PLoS One 7: e51452, 2012.
21. R Core Team. R: A language and environment for statistical computing (version 4.0.3). R Foundation for Statistical Computing, Vienna, Austria, 2020. https://www.R-project.org/. Accessed October 16, 2023.
22. Hu M, Xing L, Zhang L, Liu F, Wang S, Xie Y, Wang J, Jiang H, Guo J, Li X, *et al*: NAP1L2 drives mesenchymal stem cell senescence and suppresses osteogenic differentiation. Aging Cell 21: e13551, 2022.
23. Yang Y, Zhang W, Wang X, Yang J, Cui Y, Song H, Li W, Li W, Wu L, Du Y, *et al*: A passage-dependent network for estimating the in vitro senescence of mesenchymal stromal/stem cells using microarray, bulk and single cell RNA sequencing. Front Cell Dev Biol 11: 998666, 2023.
24. Livak KJ and Schmittgen TD: Analysis of relative gene expression data using real-time quantitative PCR and the 2(-Delta delta C(T)) method. Methods 25: 402-408, 2001.
25. Pánczél Á, Nagy SP, Farkas J, Jakus Z, Győri DS and Mócsai A: Fluorescence-based real-time analysis of osteoclast development. Front Cell Dev Biol 9: 657935, 2021.

26. Huo S, Tang X, Chen W, Gan D, Guo H, Yao Q, Liao R, Huang T, Wu J, Yang J, *et al*: Epigenetic regulations of cellular senescence in osteoporosis. Ageing Res Rev 99: 102235, 2024.
27. Qi L, Fang X, Yan J, Pan C, Ge W, Wang J, Shen SG, Lin K and Zhang L: Magnesium-containing bioceramics stimulate exosomal miR-196a-5p secretion to promote senescent osteogenesis through targeting Hoxa7/MAPK signaling axis. Bioact Mater 33: 14-29, 2023.
28. Zheng Y, Wu S, Ke H, Peng S and Hu C: Secretion of IL-6 and IL-8 in the senescence of bone marrow mesenchymal stem cells is regulated by autophagy via FoxO3a. Exp Gerontol 172: 112062, 2023.
29. Zhang W, Huang C, Sun A, Qiao L, Zhang X, Huang J, Sun X, Yang X and Sun S: Hydrogen alleviates cellular senescence via regulation of ROS/p53/p21 pathway in bone marrow-derived mesenchymal stem cells in vivo. Biomed Pharmacother 106: 1126-1134, 2018.
30. Tanaka Y, Sonoda S, Yamaza H, Murata S, Nishida K, Hama S, Kyumoto-Nakamura Y, Uehara N, Nonaka K, Kukita T and Yamaza T: Suppression of AKT-mTOR signal pathway enhances osteogenic/dentinogenic capacity of stem cells from apical papilla. Stem Cell Res Ther 9: 334, 2018.
31. Chen G, Wang S, Wei R, Liu Y, Xu T, Liu Z, Tan Z, Xie Y, Yang D, Liang Z, *et al*: Circular RNA circ-3626 promotes bone formation by modulating the miR-338-3p/Runx2 axis. Joint Bone Spine 91: 105669, 2024.
32. Jin J, Huang R, Chang Y and Yi X: Roles and mechanisms of optineurin in bone metabolism. Biomed Pharmacother 172: 116258, 2024.
33. Yin S, Lin S, Xu J, Yang G, Chen H and Jiang X: Dominoes with interlocking consequences triggered by zinc: Involvement of microelement-stimulated MSC-derived exosomes in senile osteogenesis and osteoclast dialogue. J Nanobiotechnol 21: 346, 2023.
34. Prince EW, Apps JR, Jeang J, Chee K, Medlin S, Jackson EM, Dudley R, Limbrick D, Naftel R, Johnston J, *et al*: Unraveling the complexity of the senescence-associated secretory phenotype in adamantinomatous craniopharyngioma using multimodal machine learning analysis. Neuro Oncol 26: 1109-1123, 2024.
35. Li J, Wang X, Nepovimova E, Wu Q and Kuca K: Deoxynivalenol induces cell senescence in RAW264.7 macrophages via HIF-1α-mediated activation of the p53/p21 pathway. Toxicology 506: 153868, 2024.
36. Tragoonlugkana P, Pruksapong C, Ontong P, Kamprom W and Supokawej A: Fibronectin and vitronectin alleviate adipose-derived stem cells senescence during long-term culture through the AKT/MDM2/P53 pathway. Sci Rep 14: 14242, 2024.
37. Bai L and Wang Y: Mesenchymal stem cells-derived exosomes alleviate senescence of retinal pigment epithelial cells by activating PI3K/AKT-Nrf2 signaling pathway in early diabetic retinopathy. Exp Cell Res 441: 114170, 2024.
38. Wang L, Deng Z, Li Y, Wu Y, Yao R, Cao Y, Wang M, Zhou F, Zhu H and Kang H: Ameliorative effects of mesenchymal stromal cells on senescence associated phenotypes in naturally aged rats. J Transl Med 22: 722, 2024.
39. Geng N, Xian M, Deng L, Kuang B, Pan Y, Liu K, Ye Y, Fan M, Bai Z and Guo F: Targeting the senescence-related genes MAPK12 and FOS to alleviate osteoarthritis. J Orthop Translat 47: 50-62, 2024.
40. Kohli J, Veenstra I and Demaria M: The struggle of a good friend getting old: Cellular senescence in viral responses and therapy. EMBO Rep 22: e52243, 2021.
41. Zhang H, Xu R, Li B, Xin Z, Ling Z, Zhu W, Li X, Zhang P, Fu Y, Chen J, *et al*: LncRNA NEAT1 controls the lineage fates of BMSCs during skeletal aging by impairing mitochondrial function and pluripotency maintenance. Cell Death Differ 29: 351-365, 2022.
42. Huang CY, Le HHT, Tsai HC, Tang CH and Yu JH: The effect of low-level laser therapy on osteoclast differentiation: Clinical implications for tooth movement and bone density. J Dent Sci 19: 1452-1460, 2024.
43. Zhao Y, Wang C, Qiu F, Liu J, Xie Y, Lin Z, He J and Chen J: Trimethylamine-N-oxide promotes osteoclast differentiation and oxidative stress by activating NF-κB pathway. Aging (Albany NY) 16: 9251-9263, 2024.
44. Xie X, Hu L, Mi B, Panayi AC, Xue H, Hu Y, Liu G, Chen L, Yan C, Zha K, *et al*: SHIP1 activator AQX-1125 regulates osteogenesis and osteoclastogenesis through PI3K/Akt and NF-κb signaling. Front Cell Dev Biol 10: 826023, 2022.
45. Li Y, Hu M, Xie J, Li S and Dai L: Dysregulation of histone modifications in bone marrow mesenchymal stem cells during skeletal ageing: Roles and therapeutic prospects. Stem Cell Res Ther 14: 166, 2023.
46. Shen Y, Hong Y, Huang X, Chen J, Li Z, Qiu J, Liang X, Mai C, Li W, Li X and Zhang Y: ALDH2 regulates mesenchymal stem cell senescence via modulation of mitochondrial homeostasis. Free Radic Biol Med 223: 172-183, 2024.

Copyright © 2025 Lu et al. This work is licensed under a Creative Commons Attribution-NonCommercial-NoDerivatives 4.0 International (CC BY-NC-ND 4.0) License.